



Electronic Properties of NbSe₂ over Graphene: A Meticulous Theoretical Analysis

Donald Homero Galvan, Joel Antúnez-García, Sergio Fuentes Moyado

Centro de Nanociencias y Nanotecnología, Universidad Nacional Autónoma de México, Ensenada, México

Email: donald@cny.n.unam.mx

How to cite this paper: Galvan, D.H., Antúnez-García, J. and Moyado, S.F. (2017) Electronic Properties of NbSe₂ over Graphene: A Meticulous Theoretical Analysis. *Open Access Library Journal*, 4: e3512.
<https://doi.org/10.4236/oalib.1103512>

Received: March 10, 2017

Accepted: May 8, 2017

Published: May 11, 2017

Copyright © 2017 by authors and Open Access Library Inc.

This work is licensed under the Creative Commons Attribution International License (CC BY 4.0).

<http://creativecommons.org/licenses/by/4.0/>



Open Access

Abstract

This investigation deals with a consensus electronic property analyses, for NbSe₂ over graphene using Density Functional Theory. Depending on how you construct your initial system under investigation, either starting with Armchair, Chiral or Zig-zag for a graphene layer, final different results for the electronic properties should be anticipated. It is critical to take in consideration the *brim* edges effect in the initial conditions because different final results will be obtained. Energy bands and charge density profiles will be presented for each case under study. For pristine graphene E_g (forbidden energy gap between the Valence and Conduction bands) of 0.24 eV (Armchair), 0.19 eV (Chiral) and 0.13 eV (Zig-zag) were obtained respectively. In addition, defect on the structure (vacany defect) was considered, in order to simulate a *real scenario* which could be compared to an experimental result while constructing graphene-defect-NbSe₂ system. To our knowledge, this is the first time that such a kind of investigation is presented.

Subject Areas

Modern Physics

Keywords

Density Functional Theory, Armchair, Chiral, Zig-Zag, Energy Bands

1. Introduction

Since graphene was initially synthesized in 2004 by Novozelov *et al.* [1], a great deal of research started due to its unusual electronic and magnetic properties. Due to the fact that it is considered a *zero-gap* semiconductor and presents an unusual form for conductivity due to the Dirac electrons, it is worthwhile to perform a consensus analysis for its properties. An excellent review has been

presented by Castro-Neto *et al.* [2]. Graphene is well accepted as a *zero-gap* semiconductor and presented by Wallace [3], and in addition, yields an unusual behavior when the Dirac electrons were subject to a magnetic field. This phenomenon is known as anomalous inter quantum Hall effect, first reported by Novoselov *et al.* [4] and later by Zhang *et al.* [5] [6].

On one hand, graphene has many industrial applications, to mention few of them such as: due to its ballistic electronic applications in the production of field-effect union type p-n and p-n-p materials [7], graphene quantum dots reported by Milton-Pereira *et al.* [8], Molecular detectors reported by Barraza-Jimenez, *et al.* [9] and Spin injections by Hill *et al.* [10]. On the other hand, group V Transition Metal Dichalcogenides have been studied extensively [11] [12] because they present very peculiar charge density waves (CDW) and superconductivity. 2H-NbSe₂ presents two transition temperatures T_c at 7.4 K and other at 35 K. The later is attributed to Charge Density Waves (CDW) transition. Moreover, 2H-NbSe₂ irradiated with different doses of electrons presents nanotubes of different lengths and size [13].

2. Calculations

Electronic properties were performed under Density Functional Theory, employing DMOL³ [14] program package. For each structure, geometrical optimization was performed with an energy cut off of 2.74×10^{-4} eV and a threshold of the same value was used throughout the calculations [15] [16]. For the exchange-correlation an LDA with Perdew-Burke Ernzerhof scheme was employed [17]. For the wave functions for each atomic species considered, DND basis set, which could be compared to 6 - 31 G, 6 - 31 G (d) and 6 - 31 G (d, p) Gaussian-type basis set was used. No spin-restrictions were considered, in such a way as to leave the multiplicity in automatic.

2.1. Structural Optimization

Figures 1-3 provide information regarding a propose unit cell for graphene, graphene with a NbSe₂ cluster, graphene with vacancy defect [18], and graphene with NbSe₂ cluster located over the defect for Armchair, Chiral and Zig-zag configurations. On each figure, the identification could be provided as follows: carbon atoms are grey balls, Nb with light blue balls and Se with mustard balls. Each structure was properly optimized and relaxes in such a way as to reach a minimum of energy. On each **Figures 1-3**, three rows of figures are provided. Starting from the top left hand corner, where the graphene (pristine-original) unit cell is located, continuing toward the right corner, is graphene with NbSe₂ cluster, following graphene with a defect, and last graphene with defect and NbSe₂ cluster located over the defect. In the same figures from top to bottom, the middle row of figures, a charge type of distribution (HOMO-LUMO, Highest Occupied Molecular Orbital and Lowest Unoccupied Molecular Orbital) is provided for the cases mentioned above. On the same page, last row of figures, a side view for the cases already enunciated is provided. For our analysis, let us

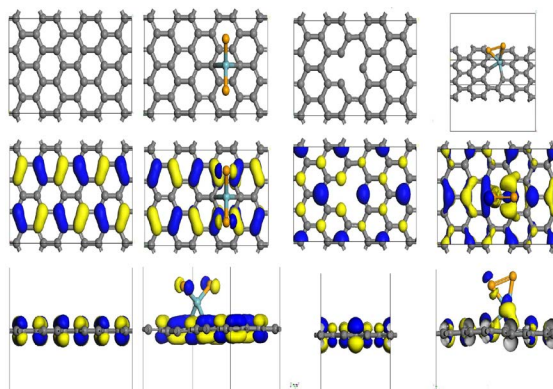


Figure 1. Distinct optimized configurations for graphene with armchair symmetry. First column corresponds to graphene (pristine), second to graphene with NbSe₂, third to graphene with defect and fourth to graphene with defect and NbSe₂. Second and third row shows (at two distinct orientations) the HOMO-LUMO distributions for the respective configurations.

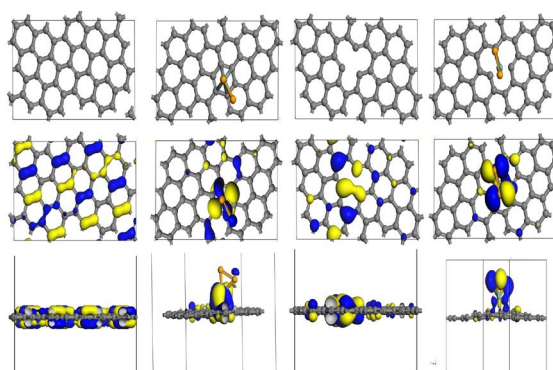


Figure 2. Distinct optimized configurations for graphene with chiral symmetry. First column corresponds to graphene (pristine), second to graphene with NbSe₂, third to graphene with defect and fourth to graphene with defect and NbSe₂. Second and third row shows (at two distinct orientations) the HOMO-LUMO distributions for the respective configurations.

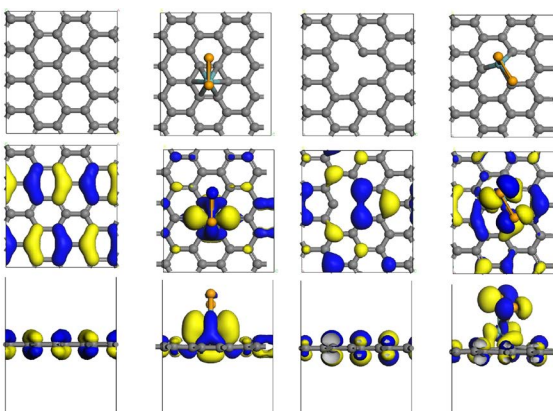


Figure 3. Distinct optimized configurations for graphene with zigzag symmetry. First column corresponds to graphene (pristine), second to graphene with NbSe₂, third to graphene with defect and fourth to graphene with defect and NbSe₂. Second and third row shows (at two distinct orientations) the HOMO-LUMO distributions for the respective configurations.

concentrate on the last row of figures for **Figure 1**, the Armchair case. Notice that the graphene (pristine) presents an almost flat charge distribution, while graphene with defect and NbSe₂ cluster yield indication that the cluster locates above two adjacent carbon atoms forming bonds in-between them. This kind of bonding is an uneven distribution.

Figure 2, provides information for the Chiral case, notice that the pristine configuration presents a different kind of charge distribution, when compared to the Armchair case, also for the graphene with defect and NbSe₂, the cluster locates by itself over the defect, but in the middle of the defect. Moreover, the bonding formed with the carbon atoms of the defect is stronger when compared with the former case. An important observation is that there is a bump and a valley for the graphene structure produced by the force exercised by the cluster. In addition, **Figure 3** provides information for a Zig-zag configuration. Notice that for graphene (pristine), charge protrudes up differently than the two former cases. Also, for graphene with defect and NbSe₂ cluster, the cluster is located above the carbon atoms forming a different kind of bonding with them when compare with the former cases.

The differences behavior encountered between the three figures could be attributed to the different form of termination (either Armchair, Chiral or Zig-zag) for each structure, the *brim concept reported in another investigations such as MoS₂* reported by our group [19] [20] in a former investigation.

2.2. Energy Bands

Due that we are interested in the electronic properties presented for the cases mentioned in the former paragraphs, energy band analyses was performed. Energy Band analysis is a powerful technique employed in order to indagate about the electronic properties (isolator, semiconductor or metal) for a material in question.

Figures 4-6 show the band structure for the former cases enunciated formerly in the manuscript. Each figure provides Energy (eV) vs. k-points, in the reciprocal space for the extended Brillouin zone, with the Fermi level (E_F) located at 0 eV. The band structure for different graphenes (**Figure 4(a)**, **Figure 5(a)** and **Figure 6(a)**) exhibit different morphology, where is evident the distinct positions along the special k-points that occupy the Dirac cones (formed at the interaction of the π and π^* bands at the Fermi surface) for each case. In **Table 1** is reported the forbidden energy gap (E_g) values and the kind of behavior presented for distinct configurations under consideration. Results show that all graphene configurations, presents a semiconductor behavior and the lower E_g value correspond to Zig-zag configuration. Interestingly no matter if a vacancy defect is practiced, or a NbSe₂ cluster is present or both in any graphene geometry, all configurations present a metallic behavior.

2.3. Total and Projected Density of States

In order to investigate the relative contributions of distinct atoms (C, Nb and Se)

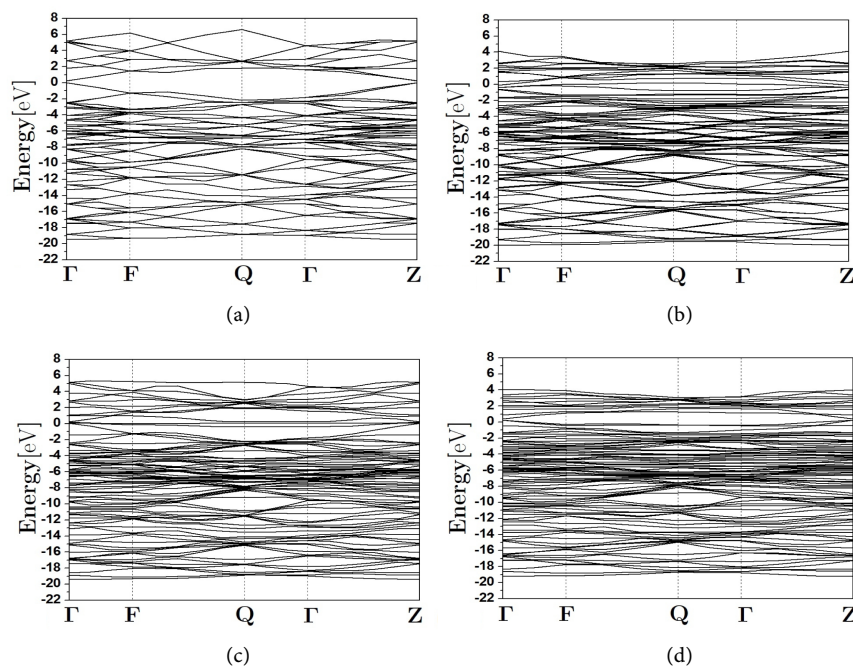


Figure 4. Energy Bands vs. K points for: (a) Graphene (pristine); (b) Graphene with NbSe₂; (c) Graphene with defect and (d) Graphene with defect and NbSe₂. Armchair configuration.

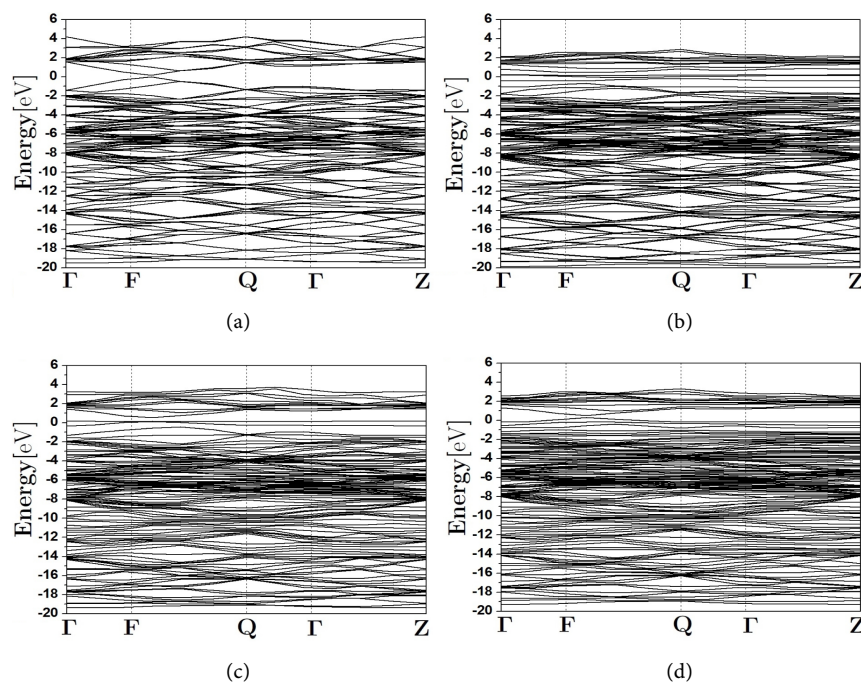


Figure 5. Energy Bands vs. K points for: (a) Graphene (pristine); (b) Graphene with NbSe₂; (c) Graphene with defect and (d) Graphene with defect and NbSe₂. Chiral configuration.

at the Fermi level, the partial density of states (PDOS) was computed for each distinct configuration. In **Figures 7(a)-(c)** vertical axis corresponds to PDOS (arbitrary units) vs information data corresponding to AI, AII, AIII and AIV

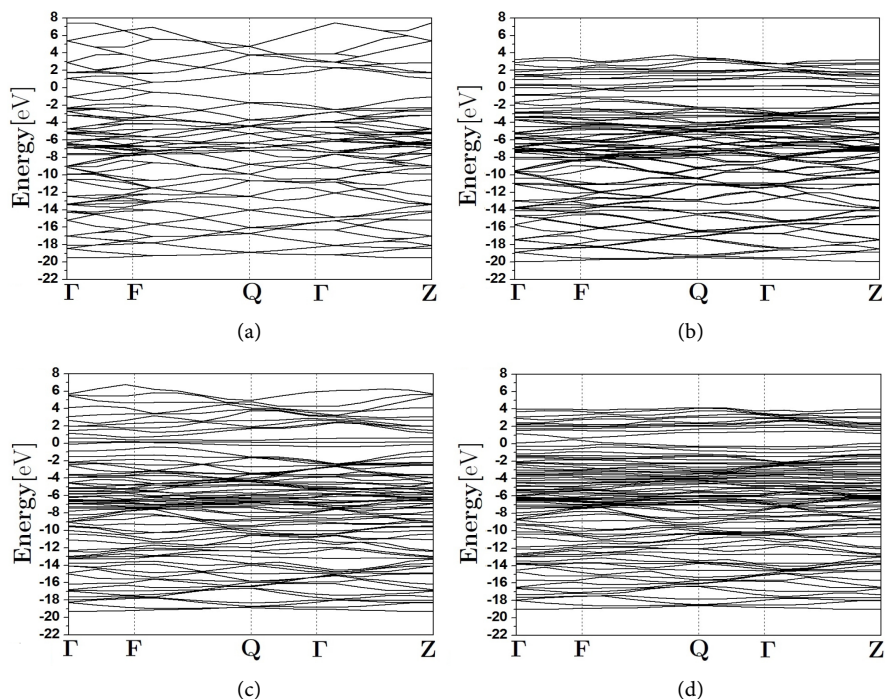
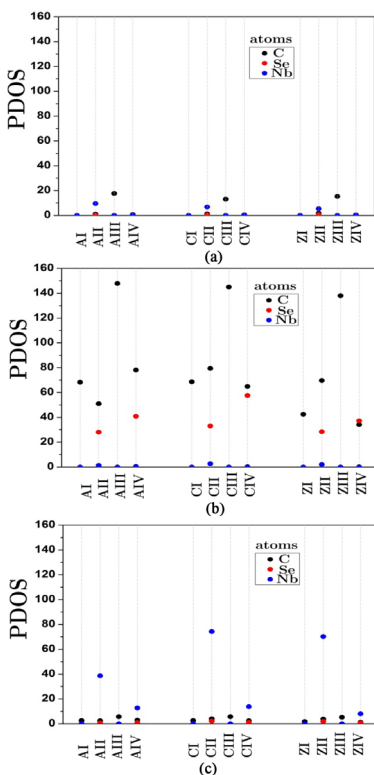


Figure 6. Energy Bands vs. K points for: (a) Graphene (pristine); (b) Graphene with NbSe₂; (c) Graphene with defect and (d) Graphene with defect and NbSe₂, Zig-zag configuration.



AI pristine
 AII Graphene-NbSe₂
 AIII Graphene-defect
 AIV Graphene-defect-NbSe₂
 A-Armchair
 C-Chirial
 Z-Zig-zag.

Figure 7. Partial Density of States (PDOS) computed at the Fermi level for: (a) s-orbital; (b) p-orbital and (c) d-orbital. A, C and Z stands for Armchair, Chiral and Zig-zag graphene geometries and I, II, III and IV are associated to pristine graphene, graphene-NbSe₂, graphene-defect and graphene-defect-NbSe₂.

Table 1. Graphene configuration (for Armchair, Chiral and Zig-zag), energy band gap (E_g in eV) and their respective behavior.

| Configuration | E_g (eV) | Behavior |
|-----------------------------------|-------------|---------------|
| Graphene | 0.24 | Semiconductor |
| Graphene-NbSe ₂ | 0.00 | Metal |
| Graphene-defect | 0.00 | Metal |
| Graphene-defect-NbSe ₂ | 0.00 | Metal |
| Graphene | 0.19 | Semiconductor |
| Graphene-NbSe ₂ | 0.00 | Metal |
| Graphene-defect | 0.00 | Metal |
| Graphene-defect-NbSe ₂ | 0.00 | Metal |
| Graphene | 0.13 | Semiconductor |
| Graphene-NbSe ₂ | 0.00 | Metal |
| Graphene-defect | 0.00 | Metal |
| Graphene-defect-NbSe ₂ | 0.00 | Metal |

(Armchair), CI, CII, CIII and CIV (Chiral) and ZI, ZII, ZIII and ZIV (Zig-zag) configurations, respectively. In each graph, “I” refer to graphene (pristine), “II” refer to graphene with a NbSe₂ cluster, “III” refer to graphene with defect while “IV” indicates graphene with defect and with a NbSe₂ cluster. In addition, contribution of distinct atoms to s, p and d orbital are shown in **Figures 7(a)-(c)** respectively. From our analysis we found that at the Fermi level, for distinct graphene configurations the Zig-zag configuration presented the lowest value for the orbitals (carbon) ratio $C[2p]/C[2d]$. On the other hand, when the contribution of distinct orbitals for the distinct configurations in **Figure 7** are compared, we observe (with exception to those the configurations that involves the presence of NbSe₂ molecule) that the metallic behavior is promoted by increasing the C[2p] orbital. For the cases that the NbSe₂ molecule is present, the deficiency of C[2p] orbital is compensated mainly by the presence of Nb[4d] and Se[4p] orbitals. Before proceed any further, it is necessary to underline that NbSe₂ crystallizes in a trigonal-prismatic configuration like MoS₂ as reported by Zonnevylle *et al.* [21], hence, due to the Crystalline Electric Field (CEF) effect, Nb d-orbitals which are five-fold degenerate, brakes the degeneracy and separate into one below two below two in energy levels. It is generally accepted that Nb d_{z^2} is the lowest in energy, while the rest are randomly arranged. On the other hand, Se[4p] orbital interact with Nb[4d] orbital of the same symmetry, producing a hybridize set of orbitals. Moreover, in the graphene honeycomb network, each Carbon atom in the hexagonal ring contributes with 4 valence electrons, from which 3 out of 4 contributes to form each ring, while one of the p-orbitals points out of the plane (p_{z^2}). This unsaturated p_{z^2} orbital from each C atom could interact with Nb d-orbital of the same symmetry which is closer to the network. Notice from **Figure 7(a)** that the contributions from s-orbitals are small when compare to the p- and d-contributions from C and Nb respectively and provided

in **Figure 7(b)** and **Figure 7(c)**. Finally, **Figure 7** shows that the participation of Nb and Se orbitals is dependent of the configuration (geometry and the presence of a defect) of a graphene sheet.

3. Conclusions

From the results obtained in this study, it is extremely important to underline the relevance for the selection of Armchair, Chiral or Zig-zag in the construction of the graphene hexagonal sheet, because that final result will be affected depending on the appropriate selection. In our case, the selection for Zig-zag graphene yielded the minimum energy of 0.13 eV for the forbidden energy gap E_g . On the other hand, we observe that the configuration of a graphene sheet affects the participation of Nb and Se orbitals.

Acknowledgements

D. H. Galvan acknowledges the Departamento de Supercomputo, Universidad Nacional Autónoma de México, Proyecto LANCAD-UNAM-DGTIC-041 for the time provided in order to perform this work.

References

- [1] Novoselov, K.S., Geim, A.K., Morozov, S.V., Jiang, D., Zhang, Y., Dubonos, S.V., Gregorova, I.V. and Firsov, A.A. (2004) Effect in Atomically Thin Carbon Film. *Science*, **306**, 666-669. <https://doi.org/10.1126/science.1102896>
- [2] Castro-Neto, A.H., Guinea, F., Peres, N.M., Novoselov, K.S. and Geim, A.K. (2009) The Electronic Properties of Graphene. *Review of Modern Physics*, **81**, 109-162. <https://doi.org/10.1103/RevModPhys.81.109>
- [3] Wallace, P.R. (1947) The Band Theory of Graphite. *Physical Review*, **71**, 622-634. <https://doi.org/10.1103/PhysRev.71.622>
- [4] Novoselov, K.S., Geim, A.K., Morozov, S.V., Jiang, D., Katsnelson, M.I., Grigorieva, I.V., Dubonos, S.V. and Firsov, A.A. (2005) Two-Dimensional Gas of Massless Dirac Fermions in Graphene. *Nature*, **438**, 197-200. <https://doi.org/10.1038/nature04233>
- [5] Zhang, Y., Tan, Y.-W., Stormer, H.L. and Kim, P. (2005) Experimental Observation of the Quantum Hall Effect and Berry's Phase in Graphene. *Nature*, **438**, 201-204. <https://doi.org/10.1038/nature04235>
- [6] Zhong, L.M. and Fogler, M.M. (2008) Nonlinear Screening and Ballistic Transport in a Graphene p-n Junction. *Physical Review Letters*, **100**, 116804.1-4.
- [7] Ossipov, A., Titov, M. and Beenaker, C.W.J. (2007) Reentrance Effect in a Graphene n-p-n Junction Coupled to a Superconductor. *Physical Review B*, **75**, 241401(R), 1-4.
- [8] Milton-Pereira Jr., J., Vasilopoulos, P. and Peeters, F.M. (2007) Tunable Quantum Dots in Bilayer Graphene. *Nano Letters*, **7**, 946-949. <https://doi.org/10.1021/nl062967s>
- [9] Barraza-Jimenez, D., Flores-Hidalgo, M.A. and Galvan, D.H. (2014) Theoretical Study of Bi Layered Graphene Use as Gas Detector. *Design and Applications of Nanomaterials for Sensors, Challenge and Advances in Computational Chemistry*, **16**, 281-287.

- [10] Hill, E.W., Geim, A.K., Novoselov, K., Schedin, F. and Blake, P. (2006) Graphene Spin Valve Devices. *IEEE Transactions on Magnetics*, **42**, 2694-2696. <https://doi.org/10.1109/TMAG.2006.878852>
- [11] Wilson, J.A. and Yoffe, A.D. (1969) The Transition Metal Dichalcogenides. Discussion and Interpretation of the Observed Optical, Electrical and Structural Properties. *Advances in Physics*, **18**, 193-335. <https://doi.org/10.1080/00018736900101307>
- [12] Henders, W.H. (1997) Dynamic and Magnetic Flux-lines in 2H-Niobium Diselenide. PhD Dissertation, New Brunswick Rutgers, The State University of New Jersey, 1-133.
- [13] Galvan, D.H., Kim, J.-H., Maple, M.B., Avalos-Borja, M. and Adem, E. (2000) Formation of NbSe₂ Nanotubes by Electron Irradiation, Fullerene. *Science Technology*, **8**, 127-151.
- [14] Software from Accelrys Inc. <http://www.accelrys.com>
- [15] Delley, B. (1990) An All-Electron Numerical Method for Solving the Local Density Functional for Polyatomic Molecules. *Journal of Chemical Physics*, **92**, 508-517. <https://doi.org/10.1063/1.458452>
- [16] Delley, B. (2000) From Molecules to Solids with DMol³. *Journal of Chemical Physics*, **113**, 7756-7764. <https://doi.org/10.1063/1.1316015>
- [17] Perdew, J.P., Burke, K. and Ernzerhof, M. (1996) Generalized Gradient Approximation Made Simple. *Physical Review Letters*, **77**, 3865-3868. <https://doi.org/10.1103/PhysRevLett.77.3865>
- [18] del Rosario Estrada Cruz, J.F. (2014) Propiedades electrónicas de nano-cúmulos de 1H-MoS₂ crecidos sobre óxido de grafeno. M.Sc. Dissertation, Programa de Posgrado en Física de Materiales, CICESE-UNAM, 10.
- [19] Galvan, D.H., Posada-Amarillas, A. and José-Yacamán, M. (2009) Metallic States at the Edge MoS₂ Clusters. *Catalysis Letters*, **132**, 323-328. <https://doi.org/10.1007/s10562-009-0132-7>
- [20] Estrada-Cruz, J., Fuentes-Moyado, S. and Galvan, D.H. (2015) Energy Bands of the 1H-MoS₂ over Reduced Graphene Oxide. *Materials Today Proceedings*, **2**, 108-112. <https://doi.org/10.1016/j.matpr.2015.04.017>
- [21] Zonnevylle, M.C. and Hoffmann, R. (1988) Thiophene Hydrodesulfurization on MoS₂; Theoretical Aspects. *Surface Science*, **199**, 320-360. [https://doi.org/10.1016/0039-6028\(88\)90415-3](https://doi.org/10.1016/0039-6028(88)90415-3)



Open Access Library

Submit or recommend next manuscript to OALib Journal and we will provide best service for you:

- Publication frequency: Monthly
- 9 [subject areas](#) of science, technology and medicine
- Fair and rigorous peer-review system
- Fast publication process
- Article promotion in various social networking sites (LinkedIn, Facebook, Twitter, etc.)
- Maximum dissemination of your research work

Submit Your Paper Online: [Click Here to Submit](#)

Or Contact service@oalib.com